Journal of General Virology (2010), **91**, 2723–2733 **DOI** 10.1099/vir.0.024109-0

Experimental evidence of recombination in murine noroviruses

Elisabeth Mathijs, Benoît Muylkens,† Axel Mauroy, Dominique Ziant, Thomas Delwiche and Etienne Thiry

Department of Infectious and Parasitic Diseases, Virology and Viral Diseases, Faculty of Veterinary Medicine, University of Liège, 4000 Liège, Belgium

Correspondence
Etienne Thiry
etienne.thiry@ulg.ac.be

Received 1 June 2010
Accepted 5 August 2010

Based on sequencing data, norovirus (NoV) recombinants have been described, but no experimental evidence of recombination in NoVs has been documented. Using the murine norovirus (MNV) model, we investigated the occurrence of genetic recombination between two co-infecting wild-type MNV isolates in RAW cells. The design of a PCR-based genotyping tool allowed accurate discrimination between the parental genomes and the detection of a viable recombinant MNV (Rec MNV) in the progeny viruses. Genetic analysis of Rec MNV identified a homologous-recombination event located at the ORF1–ORF2 overlap. Rec MNV exhibited distinct growth curves and produced smaller plaques than the wild-type MNV in RAW cells. Here, we demonstrate experimentally that MNV undergoes homologous recombination at the previously described recombination hot spot for NoVs, suggesting that the MNV model might be suitable for *in vitro* studies of NoV recombination. Moreover, the results show that exchange of genetic material between NoVs can generate viruses with distinct biological properties from the parental viruses.

INTRODUCTION

Noroviruses (NoVs) are an important cause of acute gastroenteritis in humans worldwide. Since the first description of NoVs in humans in 1968, NoV infections have also been detected in domestic and captive wild animals (Scipioni *et al.*, 2008). The genus *Norovirus* belongs to the family *Caliciviridae*. NoVs are non-enveloped viruses with a single-stranded, positive-sense, polyadenylated RNA genome composed of around 7500 nt. Three overlapping ORFs encode the non-structural (ORF1) and structural (ORF2 and ORF3) viral proteins. The ORF1-encoded polyprotein is cleaved further by the viral proteinase into six mature products with the gene order N-term, NTPase, p18–20/22, genome-linked virus protein (VPg), proteinase and polymerase (Sosnovtsev *et al.*, 2006). NoVs are divided into five genogroups (GI–V) based on their genomic composition (Zheng *et al.*, 2006). Human NoVs are classified into GI, GII and GIV, whereas bovine and murine NoVs (MNVs) cluster respectively into GIII and GV. Other NoVs detected in animals constitute distinct genotypes in GII and GIV: porcine NoVs belong to GII and NoVs detected in a lion cub and young dogs cluster into GIV (Martella *et al.*, 2007, 2008).

Little is known about human NoV biology, due to the lack of a regular cell-culture system or small-animal model for human NoVs. MNVs constitute a substitute for the *in vitro* study of human and other animal NoVs (Wobus *et al.*, 2006), as it is possible for them to be grown in murine macrophages and dendritic cell lines. Viruses can evolve rapidly due to small-scale mutations and recombination. Genetic recombination enables the creation of new combinations of genetic materials, generating more dramatic genomic changes than point mutations. This phenomenon has been described for a large number of RNA viruses (Lai, 1992). Predictive recombination tools together with similarity plots between putative recombinant genomes and the suspected parental genomes have suggested recombination at breakpoints within ORF2 in several MNV genomes (Thackray *et al.*, 2007). Although numerous human and animal recombinant NoVs have been described by phylogenetic analysis (Bull *et al.*, 2007), there is no formal or prospective evidence of recombination occurring in co-infection experiments with two NoV strains, either *in vitro* or *in vivo*.

The aim of this study was to provide experimental evidence of NoV recombination between two genetically related, cultivable MNV isolates, selected as parental isolates.

†Present address: Department of Veterinary Sciences, Physiology, Embryology and Anatomy, Faculty of Sciences, FUNDP, 5000 Namur, Belgium.

The GenBank/EMBL/DDBJ accession number for the consensus nucleotide sequence obtained for Rec MNV covering the ORF1–ORF2 junction is HM044221.

A supplementary table showing primers and probes used in the TaqMan-based discriminative PCR distinguishing between MNV-1 and WU20 is available with the online version of this paper.

Discriminative assays were set up to differentiate between the parental viruses at three loci spanning the entire genome. These assays were further used to analyse the progeny viruses recovered from different co-infections in cell culture. The biological features of the MNV recombinant generated were assessed further *in vitro* in comparison with those of the parental viruses.

RESULTS

Selection of distinguishable parental MNV isolates

Despite their biological diversity, MNV isolates described hitherto cluster into a single genogroup (Thackray *et al.*, 2007). In order to be selected as accurate MNV parental strains involved in co-infection experiments, MNV isolates should: (i) be grown in RAW cells; (ii) induce an obvious cytopathic effect in RAW cell monolayers, enabling a plaque-picking procedure for virus isolation; (iii) be related genetically to each other in order to favour homologous recombination; and (iv) bear sufficient genetic variability for discrimination. Based upon these characteristics, previously published MNV isolates MNV-1.CW1 (MNV-1) and WU20 were selected here for the study of recombination. MNV-1 is the reference MNV strain with pathogenic properties described previously in a mouse model (Karst *et al.*, 2003). WU20 is a field isolate for which pathogenic properties have not yet been determined (Thackray *et al.*, 2007). The two isolates share 87 % nucleotide sequence similarity in their complete genomes, and alignment of their full-length genomes showed maximum sequence similarity at the ORF1–ORF2 junction (Fig. 1a). To determine genetic markers enabling discrimination between MNV-1 and WU20, five RT-PCR fragments were amplified and sequenced (Table 1) from the genes encoding the N-term (locus 1), p18/VPg (locus 2), polymerase (locus 3), major capsid (locus 4) and minor capsid (locus 5) proteins (Fig. 1a). When assembled, these five fragments spanned 26.7 % of the entire genome. Alignment of respective genomic stretches obtained for MNV-1 and WU20 revealed a minimum of 11 point mutations that were used further to differentiate the virus isolates at each selected locus (Fig. 1b). Each discriminative substitution was confirmed by the alignment of five sequences of RT-PCR products obtained independently. Stability of the mutations was further established by sequencing RT-PCR fragments of MNV-1 and WU20 RNA obtained after four successive passages in cell culture (Table 1). Genetic markers were shown to be stable, as only two discriminative mutations (of the 195 detected) between MNV-1 and WU20 were lost after four passages in cell culture.

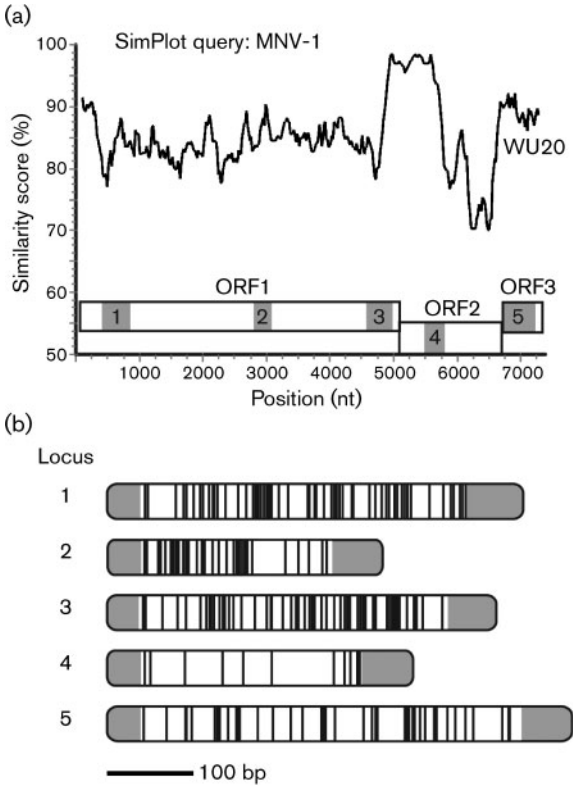

Fig. 1. Similarity plot of full-length genomes from the two parental MNV strains and genetic markers based upon point mutations. (a) SimPlot analysis. Query sequence, MNV-1; window size, 200 bp; step, 20 bp. The ordinate indicates the similarity score between MNV-1 (GenBank accession no. AY228235) and WU20 (EU004665) parental strains and the abscissa indicates the nucleotide positions. A schematic diagram drawn to scale showing the organization of MNV genome and location of the five fragments amplified by RT-PCR is shown. (b) RT-PCR sequencing assays of five amplicons accurately discriminated the two parental strains along the complete genome. Polymorphisms differentiating MNV-1 from WU20 were identified within genes encoding non-structural proteins (ORF1; N-terminal protein, p18/VPg and RNA-dependent RNA polymerase) and structural proteins (ORF2 and ORF3; major and minor capsid protein, respectively). Bars are drawn to scale and represent the five RT-PCR amplicons obtained for each genomic locus. Vertical black lines within the bars indicate the position of the nucleotide polymorphisms between MNV-1 and WU20. Areas filled in grey represent the absence of reliable sequence information due to unidirectional direct sequencing and primer sequences.

Multilocus discrimination between MNV-1 and WU20 by SYBR green- and TaqMan-based PCR assays

Isolates were genotyped at three regions across the genome: two located at the 5′ (N-term locus) and 3′ (ORF3 locus) ends of the genome and one at the polymerase region. Loci 1, 3 and 5 have been chosen for the genotyping assays, despite the fact that slight instability has been observed after four passages in regions 3 and 5. Locus 5 was preferred over locus 4 to allow the detection of potential crossovers within ORF2 or between ORF2 and ORF3. Locus 3 allowed discrimination by melt-curve analysis in SYBR green assays, as the difference in G+C content between parental viruses was sufficient (Table 1). A SYBR green genotyping assay

Table 1. Primers used for the detection of stable genetic markers in the study of recombination between two parental MNV strains, MNV-1 and WU20

The GenBank accession no. for MNV-1 is AY228235. F, Forward; R, reverse. Mixed bases in primers are as follows: Y=C or T; R=A or G.

Locus	Primer sequence (5′–3′)*	Product length (bp) (position in MNV-1)	|ΔG + C content| MNV-1−WU20 (mol%)	Nucleotide conservation after four serial passages (%)	
				MNV-1	WU20
1	**TGTAAAACGACGGCCAGT**TGAGTGGGAGGAGAGGAAG (F)	482 (260–708)	2.01	100.0	100.0
	CAGGAAACAGCTATGACCCCCTCTTCAGCCAGGTGTC (R)				
2	**TGTAAAACGACGGCCAGT**CTCCATTGATGAYTACCTCGC (F)	320 (2735–3018)	2.11	100.0	100.0
	CAGGAAACAGCTATGACCGCACAACACGGGACCAGAT (R)				
3	**TGTAAAACGACGGCCAGT**TAACCCGAGTTGACCCTGAC (F)	452 (4516–4932)	3.60	100.0	99.7
	CAGGAAACAGCTATGACCAGACACGGGAAGCCACAGT (R)				
4	**TGTAAAACGACGGCCAGT**ATTTTTCCCAARGGGTCACTC (F)	356 (5444–5763)	0.44	100.0	100.0
	CAGGAAACAGCTATGACCCTGTATCACGGGCARGTCG (R)				
5	**TGTAAAACGACGGCCAGT**CAAGCCCAGAAGGATCTCAC (F)	469 (6828–7260)	0.46	99.8	100.0
	CAGGAAACAGCTATGACCTCGTGTAGGTGCCTTGAGTC (R)				

*Sequences of standard sequencing primers (−21M13 for F and ReverseM13 for R) are indicated in bold type.

offers the advantage of being more cost-effective and easier to implement than a TaqMan-based assay. For MNV-1, the melt-curve analysis yielded a characteristic sharp peak at 90.2 °C (variation range, 89.8–90.6 °C), whereas the peak melting temperature for WU20 was 88.4 °C (variation range, 88.0–88.6 °C) (Fig. 2a). A 100 % concordance between results of DNA sequencing and T_m-shift genotyping was observed. For the N-term and ORF3 loci, two duplex TaqMan RT-PCR assays were set up for discrimination between MNV-1 and WU20. Each genome-specific probe, designed for hybridization to MNV-1 or WU20 parental viruses, was labelled at the 5′ end with a different fluorescent reporter dye (FAM and Texas red/Cy3, respectively) (see Supplementary Table S1, available in JGV Online). End-point reading of the fluorescence generated during PCR amplification demonstrated that the TaqMan assays were efficacious at discriminating MNV-1 and WU20 specifically at both loci, as shown in Fig. 2(b). DNA sequencing showed a 100 % concordance with the TaqMan PCR assay results. All real-time reactions were shown to be specific by the absence of signal when cDNAs from mock-infected RAW cells were submitted to the discriminative PCR assays. Up to 100-fold dilutions of cDNAs obtained from viral suspension titres of 10^4 p.f.u. ml^{-1} were detected successfully, showing the sensitivity of the PCRs.

Analysis of progeny viruses after MNV-1/WU20 co-infections *in vitro*

Five experiments of co-infection between MNV-1 and WU20 were performed. At least 30 progeny viruses were analysed for each co-infection scenario and were each characterized as either a parental or a recombinant virus by discriminative real-time PCR (Fig. 3a–e). Although differences in the proportion of parental genomes for progeny viruses were observed, none of the MNV-1/WU20 co-infections generated recombinant progeny viruses (Fig. 3a–e). Despite variations in the m.o.i. or the delay of infection, co-inoculation of RAW cells did not allow us to identify recombinant viruses, thereby questioning the ability of MNV-1 and WU20 to recombine in RAW cells. As a basic requirement for the exchange of genetic material between viruses is that both viruses infect a single cell simultaneously, this point was investigated further for MNV-1 and WU20 in RAW cells.

Recombinant virus detection from a co-infected cell by infectious-centre assay

An infectious-centre assay was used (i) to verify that the two virus strains were able to co-infect the same host cell, (ii) to allow further analysis of the progeny virions from a co-infected cell and (iii) to avoid the issue of dominance of one parental virus over the other. Infectious centres were selected randomly in RAW cell monolayers inoculated with a dilution of suspended RAW cells that had previously been co-inoculated by MNV-1 and WU20 at a total m.o.i. of 100 (50 each). RNA extracts from each infectious centre were

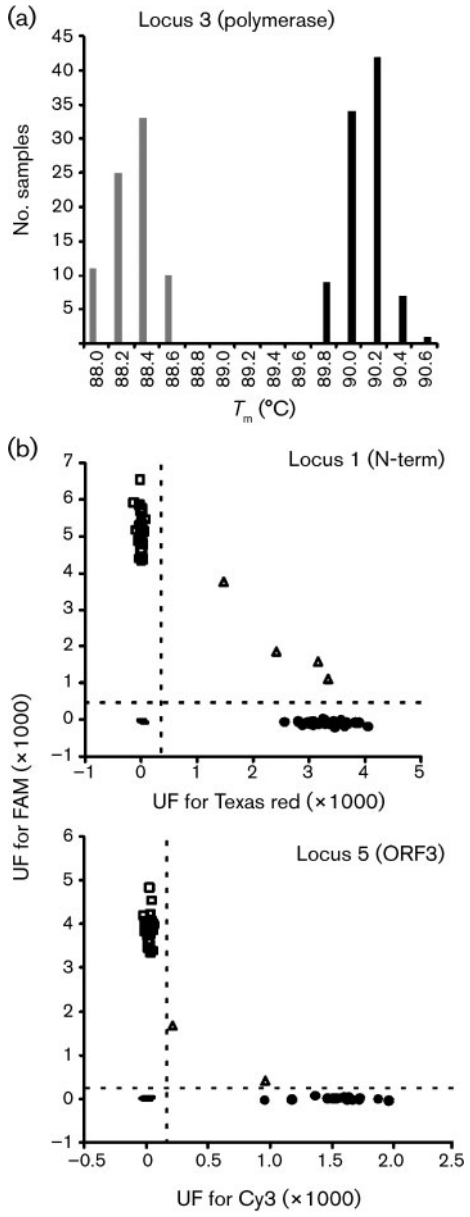

Fig. 2. SYBR green- and TaqMan-based PCR assays discriminating between MNV-1 and WU20. (a) Melt-curve analysis of SYBR green-labelled PCR products, enabling the distinction between MNV-1 (grey bars) and WU20 (black bars) genomes in the polymerase region (locus 3). Mean melting temperatures (T_m) for MNV-1 and WU20 were 90.1 ± 0.15 and 88.3 ± 0.18 °C, respectively. (b) End-point reading of the fluorescence emitted during PCR amplification of loci 1 and 5 discriminating between MNV-1 (□) and WU20 (●). Intensities of Cy3/Texas red and FAM fluorescent signals originating from WU20- and MNV-1-specific probes are plotted on the *x*- and *y*-axes, respectively. UF, Units of fluorescence; △, mixed RNA; –, non-template control and RNA extracted from mock-infected cells.

analysed further for the presence of parental genomes by the TaqMan genotyping assay targeting ORF3. In 13 of the 20 (65 %) infectious centres analysed, both MNV parental genomes were detected, indicating that single, suspended RAW cells were co-infected by MNV-1 and WU20 (Figs 3f and 4a). A total of 122 progeny viruses plaque-purified from a co-infected cell were submitted to the PCR genotyping assays at the three genomic locations described above. One virus showed discordant genotyping at the three loci (Fig. 4b–d). The WU20 signature was detected in the N-term and polymerase regions, whereas the MNV-1 signature was found in the ORF3 region. According to these observations, this progeny virion was generated following recombination occurring between loci 3 and 5 of the MNV genomes.

Genetic and phenotypic characterization of the recombinant virus

In order to confirm that recombination had occurred, the predicted recombination breakpoint of the potential recombinant MNV isolate (Rec MNV) and its parental viruses was sequenced. Alignment of the Rec MNV consensus sequence with the MNV-1 and WU20 sequences showed that the recombination breakpoint is located at the ORF1–ORF2 junction in the region of 123 bp where complete sequence identity was observed between the parental isolates (Fig. 5). Sequences of all five loci were obtained by direct sequencing for the recombinant virus and showed 100 % sequence identity to sequences from the parental viruses, being identical to WU20 for the three loci in ORF1 and to MNV-1 for loci in ORF2 and ORF3 (data not shown). Viability and sequence identities of Rec MNV were maintained during rounds of plaque purification and amplification by three serial passages in RAW cells, indicating that this study was able to generate a viable and stable recombinant virus.

In order to investigate the effect of the recombination event on viral fitness, phenotypic characteristics of Rec MNV were investigated in cell culture. Single-step growth kinetics of the recombinant and parental strains were established from three independent series. Whilst the three viruses showed similar growth curves when total and extracellular virus titres were analysed, differences were observed for intracellular virus production (Fig. 6a). For the parental viruses, intracellular virions constituted the majority of their total virus titres up to 18 h post-infection (p.i.) before extracellular titres exceeded the intracellular titres, probably due to lysis of the infected cells. In contrast, intracellular Rec MNV titres were maintained at a high level up to 24 h p.i. (Fig. 6a). Phenotypic characterization of Rec MNV was completed by plaque-size assays. In order to determine the relevance of the differences in plaque size, a non-parametric statistical method that would take into account the variation in plaque size for each virus was chosen and data were analysed with the Kolmogorov–Smirnov statistic. Results obtained from 64 randomly selected plaques for each virus indicated that Rec MNV produced significantly smaller plaques than the parental isolates, with *P*-values <0.05 (Fig. 6b, c). Taken together,

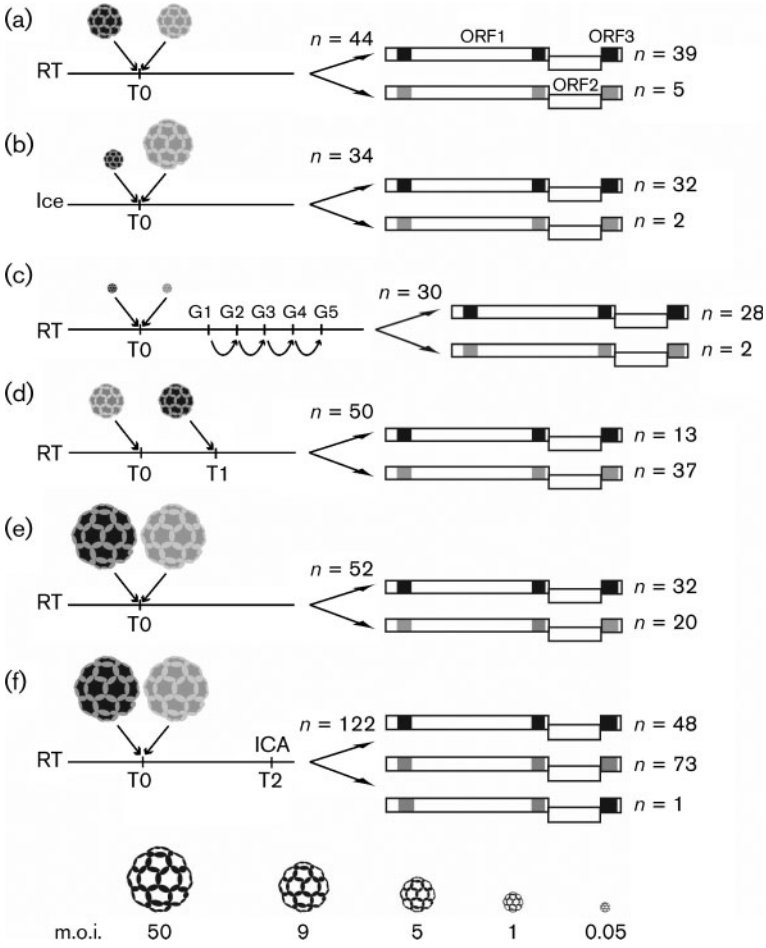

Fig. 3. Experimental schedule of MNV-1 (black)/WU20 (grey) co-infections and results of the screening of the progeny viruses based upon discriminative real-time PCR at three loci of the MNV genome. Numbers indicated above arrows are the total number of progeny viruses screened for each scenario. T0, Time zero. (a) RAW cell monolayer co-infected at an m.o.i. of 10 with an equal proportion of MNV-1 and WU20 (5/5) at room temperature (RT). (b) RAW cells co-infected at an m.o.i. of 10 (MNV-1/WU20, 1/9) on ice. (c) Co-infection at an m.o.i. of 0.1 (0.05/0.05) at RT; progeny viruses were analysed at generation 5 (G5). (d) RAW cells were infected at RT with WU20 at an m.o.i. of 5 followed 1 h later (T1) by superinfection with MNV-1 at an m.o.i. of 5. (e) Co-infection at RT at an m.o.i. of 100 (50/50). (f) Co-infection at RT at an m.o.i. of 100 (50/50) followed by an infectious-centre assay (ICA) at T2. In all scenarios, progeny viruses were analysed from whole-flask lysates at the first generation (G1) except in (c), where progeny viruses were analysed at G5, and (f), where progeny viruses were analysed from a co-infected infectious-centre lysate.

these results indicate that, although similar total virus titres were obtained for all three viruses, Rec MNV seemed to be sequestered longer inside the cell before release. This longer cell association may reduce the spread of Rec MNV to neighbouring cells, thus explaining the smaller plaques.

DISCUSSION

Although phylogenetic analyses have suggested genetic recombination in NoVs (Bull *et al.*, 2007), NoV recombinants have not been identified previously from co-infected cultured cells. Here, using the MNV model, we provide the first experimental evidence of MNV-1 recombination by co-inoculation of two distinguishable parental MNV isolates in RAW cells. Similarly to what has been observed previously for field NoV recombinant viruses (Bull *et al.*, 2005), the crossover region identified in Rec MNV was mapped to a homologous region between the parental MNV-1 and WU20 genomes located at the ORF1–ORF2 junction. Furthermore, our data show that a NoV recombination event yielded a recombinant virus exhibiting biological properties that differ from the parental ones.

In order to provide experimental evidence of recombination between two MNV isolates, we developed a new protocol based on PCR genotyping assays targeting three regions across the entire MNV genome. This tool constitutes a highly sensitive, specific, rapid and robust method for discrimination between the parental viral genomes. Single nucleotide polymorphism (SNP) genotyping assays have recently been validated for use as reliable recombination markers for the study of recombination between two closely related DNA viruses (Muylkens *et al.*, 2009). Here, their use enabled the detection of a recombinant MNV generated *in vitro* and this type of assay would therefore be suitable for *in vivo* MNV recombination studies.

In this study, a chimeric WU20–MNV-1 virus was recovered from one of six permissive co-infection assays in which a total of 332 plaque-isolated progeny viruses were analysed. At an initial m.o.i. of 100 with equal proportions of parental MNV genomes, in contrast to results for whole-flask lysate, analysis by genotyping of viruses from a co-infected infectious-centre lysate allowed the detection of a recombinant virus. Thus, the use of an infectious-centre assay may be required for the detection of recombinant MNVs. Recombination frequencies estimated for other RNA viruses need to be interpreted with care, as there are great disparities between experimental set-ups of *in vitro* RNA recombination studies, and rates vary between

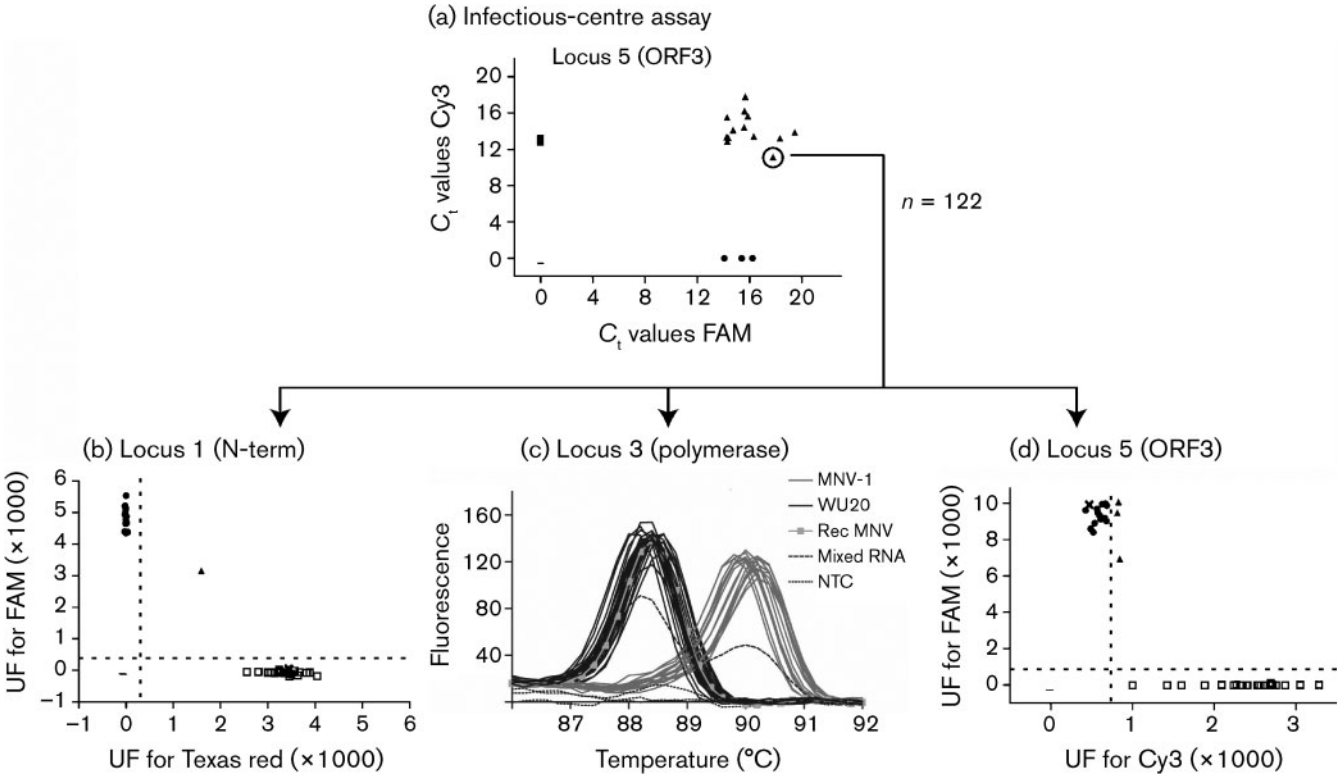

Fig. 4. Detection of a recombinant MNV from a co-infected cell determined by an infectious-centre assay. (a) Twenty infectious centres were selected randomly from RAW cell monolayers previously co-infected by MNV-1 (●) and WU20 (■) at a total m.o.i. of 100 (50 each). ▲, Mixed RNA; NTC, non-template control (–). Both parental genomes could be detected in 13 of 20 infectious centres. Of 122 progeny viruses from one co-infection scenario that were genotyped by PCR in three genomic regions [N-term (b), polymerase (c) and ORF3 (d)], only one virus (Rec MNV; ×) showed discordant genotyping in the three regions. C_t, Threshold cycle; UF, units of fluorescence.

0.13 and 2 % for picornaviruses (Cooper, 1968; Kirkegaard & Baltimore, 1986; McCahon & Slade, 1981). Also, most recombination experiments performed with RNA positive-strand viruses have been designed under extreme positive selection (e.g. with temperature-sensitive, guanidine-resistant or poorly replicative viruses being used as parental viruses) to allow the detection of rare recombination events *in vitro* (Giraudo *et al.*, 1988; Spann *et al.*, 2003). In our study, the MNV recombination frequency obviously exceeded reversion rates and was sufficiently high for the detection of a recombinant genome in the absence of selection pressure. Therefore, NoV recombination rates could be higher than those of other positive-sense RNA viruses. This finding is consistent with the great amount of data available for field NoV recombinant strains based upon sequence analysis (Ambert-Balay *et al.*, 2005; Bull *et al.*, 2007; Jiang *et al.*, 1999; Martella *et al.*, 2009; Mauroy *et al.*, 2009). We are aware that our results might not reflect the actual frequency of crossover between the parental genomes because our method relies upon multiple virus-amplification steps, which only enable the identification of replication-effective recombinants. Moreover, homologous recombination involves genomic transfer between viruses with significant sequence similarity (Kirkegaard & Baltimore, 1986; Meurens *et al.*, 2004), indicating that co-infections of MNV genomes with higher nucleotide identities than the parental genomes used in the present study might yield more recombinant viruses. All in all, on the proviso that the method is optimized further for the generation of recombinants, MNV constitutes a valuable study model for *in vitro* and *in vivo* NoV recombination.

Homologous recombination has been described for a wide range of RNA and DNA viruses (Lai, 1992; Spann *et al.*, 2003; Thiry *et al.*, 2005). A copy-choice mechanism in which the viral RNA polymerase switches templates during RNA synthesis seems to account for the majority of RNA virus recombinants (Lai, 1992). In the present study, the recombination crossover for Rec MNV has been shown to lie near the ORF1–ORF2 junction, but we were unable to define the point more precisely due to the perfect identity between parental strains across 123 bp in this region. Recombination hot spots have also been found in other RNA viruses, including poliovirus, brome mosaic virus and retroviruses (Fan *et al.*, 2007; Nagy & Simon, 1997; Tolskaya *et al.*, 1987). Such hot spots are either sequence-dependent

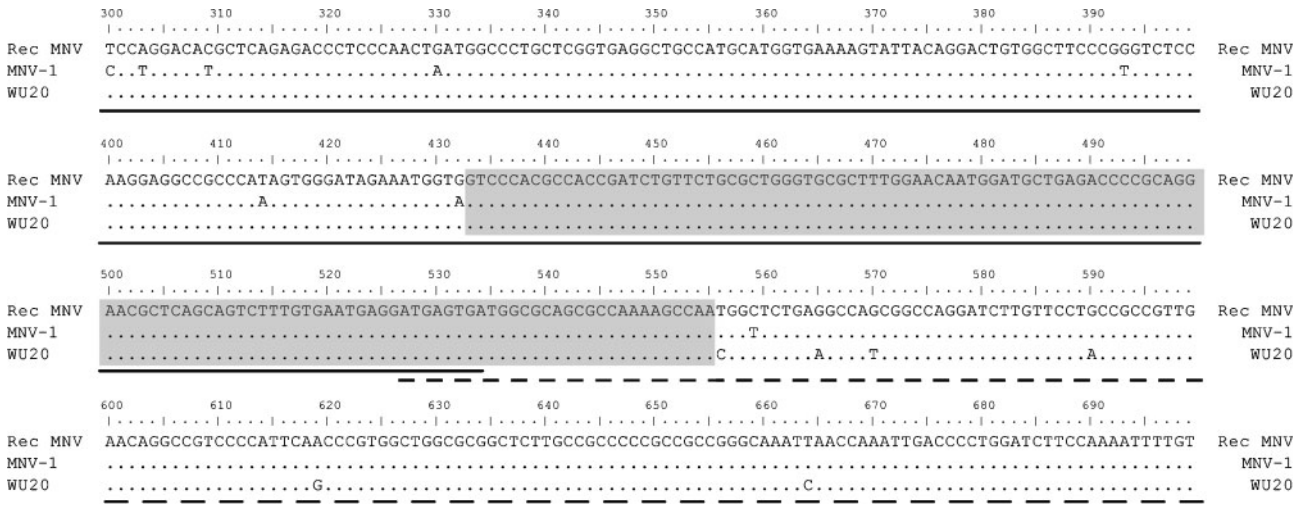

Fig. 5. Sequence alignment of a 1530 bp fragment covering the ORF1–ORF2 junction of MNV recombinant (Rec MNV) and parental (MNV-1 and WU20) viruses. Nucleotide identities with the upper sequence are represented by dots. The boxed grey area represents the region (123 bp) that potentially served as breaking point in the RNA recombination event. Sequences corresponding to the 3′ end of ORF1 and the 5′ end of ORF2 are indicated by a continuous and a dashed line, respectively.

or associated with RNA secondary structures. Sequence analysis of field NoV, sapovirus and feline calicivirus recombinants has stipulated the ORF1–ORF2 junction to be a preferential breakpoint for recombination (Bull *et al.*, 2005; Coyne *et al.*, 2006; Hansman *et al.*, 2005). Indeed, this region has been shown to exhibit a marked suppression of synonymous variability that coincides precisely with stem–loop RNA secondary structures on the anti-genomic strand upstream of a subgenomic transcript within each genus of the family *Caliciviridae*, including MNV (Simmonds *et al.*, 2008). In the present study, when the anti-genomic RNA sequence of the homologous region, including the crossover point between MNV-1 and WU20, was submitted for RNA secondary-structure prediction, a similar stem–loop structure was observed (data not shown). This suggests that viral RNA secondary structures in this region may enhance RNA recombination in MNV, as they are predicted either to hold recombination sites in close proximity, acting as a 'handle' for the RNA-dependent RNA polymerase to grab the acceptor strand, or to contribute to polymerase pausing. Thus, our data provide some experimental evidence in support of the recombination model for NoVs proposed by Bull *et al.* (2005). Phylogenetic shifts, probably due to recombination events, have been described previously in MNV genomes (Thackray *et al.*, 2007). In contrast to our observation, most of the predicted crossover sites were located in ORF2 or at the ORF2–ORF3 junction. One explanation for this discrepancy could be that recombination hot spots might differ depending on experimental or field conditions. Also, convergent evolution could be responsible for phylogenetic disagreement among MNV sequences. Additional experimental and field data will be needed to identify MNV recombination hot spots.

RNA recombination is thought to be a major driving force in virus evolution (Worobey & Holmes, 1999). In this study, phenotypic characteristics of Rec MNV were investigated in cell culture in order to understand the biological benefits caused by recombination. Plaque-size analysis together with intracellular growth-curve kinetics of Rec MNV, in comparison with those of the parental viruses, indicated a reduction in fitness *in vitro*, probably due to less efficient virus egress. However, an effect due to a different cell-passage history could not be ruled out because changes in virus phenotypes have previously been observed throughout subsequent cell passaging (Wobus *et al.*, 2004). The altered phenotype of Rec MNV could be explained by the fact that viral processes could be influenced by suboptimal interactions between the non-structural proteins and the structural proteins acquired from each parental virus. Evidence based on recombinants generated from a small, ssDNA virus, maize streak virus, demonstrated that fragments of genetic material only function optimally if they reside within genomes similar to those in which they evolved (Martin *et al.*, 2005). Observations made for field NoV recombinants may indicate that shifts between NoV genomic materials could generate viruses with increased virulence in hosts. From 2000 to 2002, sporadic cases as well as outbreaks of gastroenteritis were linked with recombinant NoV GIIb variants throughout Europe (Ambert-Balay *et al.*, 2005; Reuter *et al.*, 2006). Later, GIIb recombinants were identified in a wide range of countries, indicating their widespread distribution across continents (Bruggink & Marshall, 2009; Fukuda *et al.*, 2008; Gomes *et al.*, 2007). It is possible that recombination was able to give rise to novel NoV strains capable of epidemic spread in human

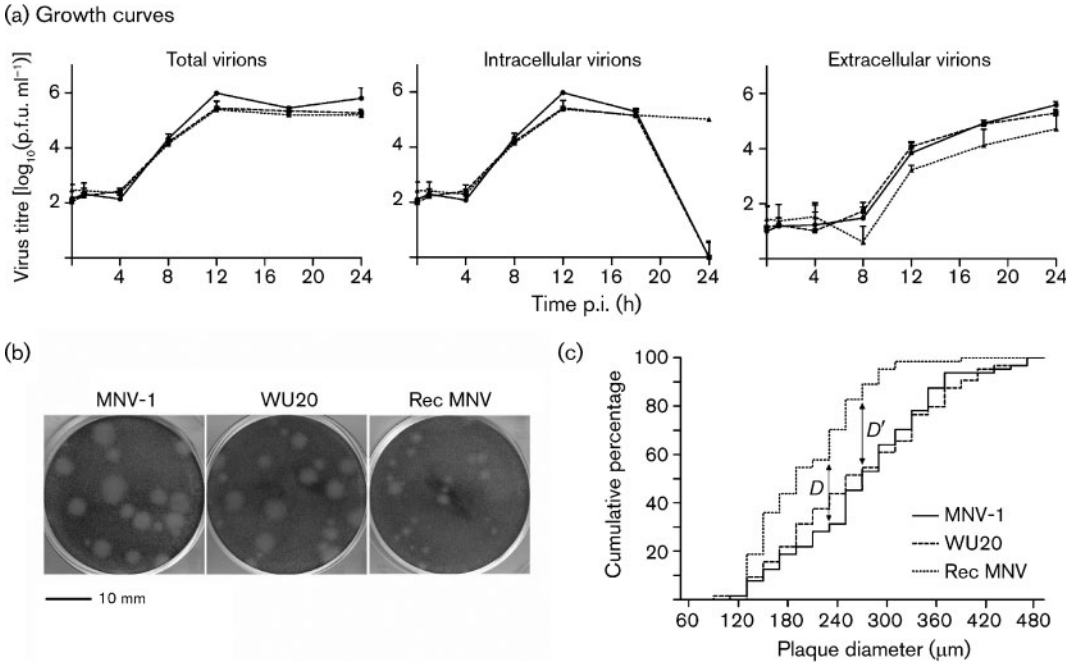

Fig. 6. *In vitro* growth properties of Rec MNV. (a) Single-step growth kinetics of MNV-1 (●), WU20 (■) and Rec MNV (▲). Data for total, intracellular and extracellular MNV virions were obtained after infection of RAW 264.7 cells at an m.o.i. of 5. Virus titres, expressed as p.f.u., are means + SD of triplicates. (b) RAW cell monolayers were infected with dilutions of MNV-1, WU20 and Rec MNV (passages 5, 4 and 3, respectively) and processed by plaque assay. Cells were fixed by adding 4 % formaldehyde and plaques were visualized with crystal violet staining. Pictures were taken of wells with dilutions showing individual plaques. (c) Plaque sizes of Rec MNV were compared with the parental ones by Kolmogorov–Smirnov statistic. From a total of 64 randomly selected plaques measured in each virus population, the cumulative percentage of plaques within increasing diameter ranges was calculated. Data were plotted with the diameter values of plaque size on the *x*-axis and the cumulative percentage on the *y*-axis. Rec MNV was compared with its parental strains by calculating maximum absolute difference (D_{max}) between the cumulative percentage of Rec MNV and its parental strains MNV-1 and WU20 (referred to as *D* and *D′*, respectively). Two-tailed *P*-values were used to determine the level of significance between the compared populations (Muylkens *et al.*, 2006). The *D* calculated for Rec MNV/MNV-1 gave a *P*-value <0.0001, and the *D′* for Rec MNV/WU20 gave a *P*-value <0.0011. For MNV-1/WU20, the D_{max} value gave a *P*-value of 0.9497.

populations. This study provides experimental proof for the acquisition of novel biological properties of an MNV that had undergone recombination. The effect of recombination upon the virulence of recombinant viruses needs be evaluated through *in vivo* studies in mice, the natural host of MNV.

In conclusion, a recombinant virus was generated by co-inoculation of RAW cells with two distinguishable MNV isolates in the absence of selection markers. The MNV model appears to be suitable for the study of NoV recombination in cell culture in the absence of available culture systems for human NoVs. Additional *in vitro* and *in vivo* studies would enable further insights into NoV genetic-diversifying mechanisms such as recombination.

METHODS

Viruses and cells. MNV isolates [MNV-1.CW1 and WU20 (Thackray *et al.*, 2007)] were propagated in RAW 264.7 cells (ATCC TIB-71) grown in Dulbecco's modified Eagle's medium (Invitrogen) complemented (DMEMc) with 10 % heat-inactivated FCS (BioWhittaker), 2 % penicillin (5000 U ml^{-1}) and streptomycin (5000 μg ml^{-1}) (PS; Invitrogen) and 1 % HEPES buffer (1 M; Invitrogen).

Virus stocks were produced by infection of RAW cells at an m.o.i. of 0.05. Two days p.i., cells and medium were harvested and clarified by centrifugation for 20 min (1000 ***g***) after two freeze/thaw cycles. Supernatants were purified by ultracentrifugation on a 30 % sucrose cushion in an SW28 rotor (Beckman Coulter) at 25 000 r.p.m. for 4 h at 4 °C. Pellets were resuspended in PBS, aliquotted and frozen at −80 °C.

Plaque assay and plaque purification of MNV isolates. Titres of each virus production were determined by plaque assay as described by Hyde *et al.* (2009). MNV isolates were plaque-purified three times following a plaque-picking method adapted from the plaque-assay method.

Co-infection experiments. Monolayers of RAW cells prepared in 25 cm^2 flasks (6.5×10^6 cells) were infected by MNV-1, WU20 or both viruses at an m.o.i. of 10. Further co-infections were performed under different conditions. Briefly, co-infections were carried out

either at room temperature or on ice. Different m.o.i.s of each parental virus for co-infection were used and supernatants were collected for analysis either after 24 h or after five serial passages. Finally, superinfection of MNV-1 upon WU20 with a 1 h delay was performed. After 1 h infection, inocula were removed and cells were washed thoroughly with sterile PBS before the addition of fresh medium. Forty-eight hours after infection, cells and medium were harvested and clarified after two freeze/thaw cycles.

Isolation and screening of progeny viruses. A plaque assay for virus isolation was set up by modifying the protocol described by Hyde *et al.* (2009). Briefly, RAW 264.7 monolayers cultured in six-well plates (1.5×10^6 cells per well) were infected with 1 ml of the appropriate dilution per well at room temperature. After 1 h, the inoculum was removed and cells were overlaid with 2 ml medium containing 70 % DMEM-Glutamax (4.5 g glucose l^{-1} and 15 mM sodium hydrogen carbonate), 2.5 % FCS, 2 % PS, 1 % HEPES and 0.7 % SeaPlaque agarose (Lonza). After 2 days incubation at 37 °C with 5 % CO_2, cells were stained for visualization by adding 2 ml minimum essential medium (Invitrogen)/1 % low-melting-point agarose containing 0.01 % neutral red. Individual plaques were picked and propagated by inoculation onto RAW cells grown in 24-well plates. After 72 h (a time corresponding to the cytopathic effect generated by plaque-purified isolates), supernatants were collected and frozen at −80 °C before further analysis.

Infectious-centre assay. In order to determine whether RAW cells were infected by both MNV strains, an infectious-centre assay was carried out with a 50 : 50 mixture of MNV-1 and WU20 at an m.o.i. of 100 as described by Chuang & Chen (2009). After 2 days, viruses from infectious centres (plaques) were isolated and virus infection was verified by genome amplification by a discriminative TaqMan-based PCR as described below.

Viral RNA preparation, RT-PCR and sequencing. Viral RNA from parental and progeny viruses was extracted from 100 µl supernatant of MNV-infected RAW cells with an RNeasy mini kit (Qiagen) according to the manufacturer's instructions. RNA extracts were stored at −80 °C until use. Five fragments of 300–600 bp were amplified with hybrid primers, specific to the viral sequence and harbouring the sequence of the M13 forward and reverse primers at their 5′ end (Vende *et al.*, 1995) (Table 1). First-stranded cDNA was generated by an iScript cDNA Synthesis kit (Bio-Rad). PCRs were carried out on 3 µl cDNA in 50 µl nuclease-free water containing 300 nM of both forward and reverse primers, 0.1 mM dNTPs, 2.5 % DMSO, 20 mM Tris/HCl, 10 mM $(NH_4)_2SO_4$, 10 mM KCl, 2 mM $MgSO_4$, 0.1 % Triton X-100 and 1 U *Taq* DNA Polymerase (New England Biolabs). Two successive PCR-amplification cycles with distinct annealing temperatures were performed as described by Vende *et al.* (1995). Amplicons were visualized by electrophoresis and purified by ethanol precipitation. Direct sequencing of PCR products was carried out by GATC Biotech sequencing facilities (Konstanz, Germany) with reverse primer M13 using an ABI 3730xl DNA Analyzer (Applied Biosystems). In order to obtain sequences covering the ORF1–ORF2 junction, PCR was performed with the forward primer from locus 3 and the reverse primer from locus 4 in order to amplify a 1578 bp long fragment. The reaction was carried out with iProof High Fidelity DNA polymerase (Bio-Rad) on 2 µl cDNA in a reaction volume of 50 µl according to the manufacturer's instructions. After purification, fragments were cloned into a pGEM-T Easy cloning vector (Promega) before being sequenced in both directions at GATC Biotech sequencing facilities (Konstanz, Germany).

Virus discrimination. For locus 3, a SYBR green assay with the hybrid primer pair 3 in the polymerase region was implemented (Table 1). One microlitre of cDNA was added to a 20 µl reaction volume containing 10 µl iQ SYBR Green Supermix (Bio-Rad), 10 pmol each of forward and reverse primers and 9.5 µl nuclease-free water. The PCR-amplification protocol consisted of 3 min at 95 °C, followed by 35 cycles of 10 s at 95 °C, 45 s at 50 °C and 45 s at 72 °C.

For the N-term and ORF3 regions (loci 1 and 3), a multiplex TaqMan real-time PCR was developed for discrimination between MNV-1 and WU20 based upon SNPs in the sequences targeted by fluorogenic TaqMan oligoprobes (Supplementary Table S1). One microlitre of cDNA was added to a 20 µl reaction volume containing 10 µl of iQ Supermix (Bio-Rad). Final concentrations of primers and probes are indicated in Supplementary Table S1. Amplification cycles were performed as follows: 5 min at 95 °C, followed by 30 cycles of 10 s at 95 °C and 40 s at 60 °C.

Bioinformatics. Sequence analyses and alignments were carried out in the BioEdit Sequence Editor software version 7.0.9.0 (Hall, 1999). Complete-genome sequence-similarity analysis was performed by using SimPlot software, available at http://sray.med.som.jhmi.edu/SCRoftware/simplot (Lole *et al.*, 1999). G+C content analysis was performed using CPGPLOT software (http://bioweb.pasteur.fr/docs/EMBOSS/cpgplot.html) (Larsen *et al.*, 1992).

One-step virus growth analysis and plaque-size determination. RAW cells cultured in 24-well plates were infected by the respective viruses at an m.o.i. of 5. After 1 h incubation on ice, the inoculum was removed and the cells were washed three times with PBS to remove unbound virus, followed by the addition of DMEMc. Plates were incubated at 37 °C for the stated length of time; time zero indicates the time at which the medium was added. After 0, 1, 4, 8, 12, 18 and 24 h incubation, an aliquot of the culture medium was removed and, together with infected cell monolayers, frozen at −80 °C. Virus titres were determined by plaque assay as described by Hyde *et al.* (2009). Plaque surfaces and diameters were determined with the ImageJ Java-based image-processing program (http://rsb.info.nih.gov/ij/).

Statistical analysis. The plaque sizes of Rec MNV were compared with the parental ones by the Kolmogorov–Smirnov statistic (Lilliefors, 1967; Muylkens *et al.*, 2006).

GenBank accession number. The consensus nucleotide sequence obtained for Rec MNV covering the ORF1–ORF2 junction was deposited in GenBank/EMBL/DDBJ under the accession no. HM044221.

ACKNOWLEDGEMENTS

We thank Professor Herbert Virgin and Dr Larissa Thackray (Washington University, St Louis, MO, USA) for providing the MNV isolates and RAW 264.7 cells; Professor Mieke Uyttendaele, Dr Leen Baert and Ambroos Stals for their help with MNV cell culture and virus production; and Professor Nadine Antoine for her contribution to plaque-size determination. This study was supported by grants from the Belgian Science Policy 'Science for a Sustainable Development' (SD/AF/01), the Fonds de la Recherche Scientifique (FRS-FNRS) (2.4624.09) and the University of Liège 'Fonds speciaux pour la Recherche-crédits classiques' 2008–2009 (C-09/60).

REFERENCES

Ambert-Balay, K., Bon, F., Le Guyader, F., Pothier, P. & Kohli, E. (2005). Characterization of new recombinant noroviruses. *J Clin Microbiol* **43**, 5179–5186.

Bruggink, L. D. & Marshall, J. A. (2009). Molecular and epidemiological features of GIIb norovirus outbreaks in Victoria, Australia, 2002–2005. *J Med Virol* **81**, 1652–1660.

Bull, R. A., Hansman, G. S., Clancy, L. E., Tanaka, M. M., Rawlinson, W. D. & White, P. A. (2005). Norovirus recombination in ORF1/ORF2 overlap. *Emerg Infect Dis* **11**, 1079–1085.

Bull, R. A., Tanaka, M. M. & White, P. A. (2007). Norovirus recombination. *J Gen Virol* **88**, 3347–3359.

Chuang, C. K. & Chen, W. J. (2009). Experimental evidence that RNA recombination occurs in the Japanese encephalitis virus. *Virology* **394**, 286–297.

Cooper, P. D. (1968). A genetic map of poliovirus temperature-sensitive mutants. *Virology* **35**, 584–596.

Coyne, K. P., Reed, F. C., Porter, C. J., Dawson, S., Gaskell, R. M. & Radford, A. D. (2006). Recombination of Feline calicivirus within an endemically infected cat colony. *J Gen Virol* **87**, 921–926.

Fan, J., Negroni, M. & Robertson, D. L. (2007). The distribution of HIV-1 recombination breakpoints. *Infect Genet Evol* **7**, 717–723.

Fukuda, S., Sasaki, Y., Takao, S. & Seno, M. (2008). Recombinant norovirus implicated in gastroenteritis outbreaks in Hiroshima Prefecture, Japan. *J Med Virol* **80**, 921–928.

Giraudo, A. T., Gomes, I., de Mello, P. A., Beck, E., La Torre, J. L., Scodeller, E. A. & Bergmann, I. E. (1988). Behavior of intertypic recombinants between virulent and attenuated aphthovirus strains in tissue culture and cattle. *J Virol* **62**, 3789–3794.

Gomes, K. A., Stupka, J. A., Gomez, J. & Parra, G. I. (2007). Molecular characterization of calicivirus strains detected in outbreaks of gastroenteritis in Argentina. *J Med Virol* **79**, 1703–1709.

Hall, T. A. (1999). BioEdit: a user friendly biological sequence alignment editor and analysis program for Windows 95/98/NT. *Nucleic Acids Symp Ser* **41**, 95–98.

Hansman, G. S., Takeda, N., Oka, T., Oseto, M., Hedlund, K. O. & Katayama, K. (2005). Intergenogroup recombination in sapoviruses. *Emerg Infect Dis* **11**, 1916–1920.

Hyde, J. L., Sosnovtsev, S. V., Green, K. Y., Wobus, C., Virgin, H. W., IV & Mackenzie, J. M. (2009). Mouse norovirus replication is associated with virus-induced vesicle clusters originating from membranes derived from the secretory pathway. *J Virol* **83**, 9709–9719.

Jiang, X., Espul, C., Zhong, W. M., Cuello, H. & Matson, D. O. (1999). Characterization of a novel human calicivirus that may be a naturally occurring recombinant. *Arch Virol* **144**, 2377–2387.

Karst, S. M., Wobus, C. E., Lay, M., Davidson, J. & Virgin, H. W., IV (2003). STAT1-dependent innate immunity to a Norwalk-like virus. *Science* **299**, 1575–1578.

Kirkegaard, K. & Baltimore, D. (1986). The mechanism of RNA recombination in poliovirus. *Cell* **47**, 433–443.

Lai, M. M. (1992). RNA recombination in animal and plant viruses. *Microbiol Rev* **56**, 61–79.

Larsen, F., Gundersen, G., Lopez, R. & Prydz, H. (1992). CpG islands as gene markers in the human genome. *Genomics* **13**, 1095–1107.

Lilliefors, H. W. (1967). On the Kolmogorov–Smirnov test for normality with mean and variance unknown. *J Am Stat Assoc* **62**, 399–402.

Lole, K. S., Bollinger, R. C., Paranjape, R. S., Gadkari, D., Kulkarni, S. S., Novak, N. G., Ingersoll, R., Sheppard, H. W. & Ray, S. C. (1999). Full-length human immunodeficiency virus type 1 genomes from subtype C-infected seroconverters in India, with evidence of intersubtype recombination. *J Virol* **73**, 152–160.

Martella, V., Campolo, M., Lorusso, E., Cavicchio, P., Camero, M., Bellacicco, A. L., Decaro, N., Elia, G., Greco, G. & other authors (2007). Norovirus in captive lion cub (*Panthera leo*). *Emerg Infect Dis* **13**, 1071–1073.

Martella, V., Lorusso, E., Decaro, N., Elia, G., Radogna, A., D'Abramo, M., Desario, C., Cavalli, A., Corrente, M. & other authors (2008). Detection and molecular characterization of a canine norovirus. *Emerg Infect Dis* **14**, 1306–1308.

Martella, V., Decaro, N., Lorusso, E., Radogna, A., Moschidou, P., Amorisco, F., Lucente, M. S., Desario, C., Mari, V. & other authors (2009). Genetic heterogeneity and recombination in canine noroviruses. *J Virol* **83**, 11391–11396.

Martin, D. P., van der Walt, E., Posada, D. & Rybicki, E. P. (2005). The evolutionary value of recombination is constrained by genome modularity. *PLoS Genet* **1**, e51.

Mauroy, A., Scipioni, A., Mathijs, E., Thys, C. & Thiry, E. (2009). Molecular detection of kobuviruses and recombinant noroviruses in cattle in continental Europe. *Arch Virol* **154**, 1841–1845.

McCahon, D. & Slade, W. R. (1981). A sensitive method for the detection and isolation of recombinants of foot-and-mouth disease virus. *J Gen Virol* **53**, 333–342.

Meurens, F., Keil, G. M., Muylkens, B., Gogev, S., Schynts, F., Negro, S., Wiggers, L. & Thiry, E. (2004). Interspecific recombination between two ruminant alphaherpesviruses, bovine herpesviruses 1 and 5. *J Virol* **78**, 9828–9836.

Muylkens, B., Meurens, F., Schynts, F., de Fays, K., Pourchet, A., Thiry, J., Vanderplasschen, A., Antoine, N. & Thiry, E. (2006). Biological characterization of bovine herpesvirus 1 recombinants possessing the vaccine glycoprotein E negative phenotype. *Vet Microbiol* **113**, 283–291.

Muylkens, B., Farnir, F., Meurens, F., Schynts, F., Vanderplasschen, A., Georges, M. & Thiry, E. (2009). Coinfection with two closely related alphaherpesviruses results in a highly diversified recombination mosaic displaying negative genetic interference. *J Virol* **83**, 3127–3137.

Nagy, P. D. & Simon, A. E. (1997). New insights into the mechanisms of RNA recombination. *Virology* **235**, 1–9.

Reuter, G., Vennema, H., Koopmans, M. & Szucs, G. (2006). Epidemic spread of recombinant noroviruses with four capsid types in Hungary. *J Clin Virol* **35**, 84–88.

Scipioni, A., Mauroy, A., Vinje, J. & Thiry, E. (2008). Animal noroviruses. *Vet J* **178**, 32–45.

Simmonds, P., Karakasiliotis, I., Bailey, D., Chaudhry, Y., Evans, D. J. & Goodfellow, I. G. (2008). Bioinformatic and functional analysis of RNA secondary structure elements among different genera of human and animal caliciviruses. *Nucleic Acids Res* **36**, 2530–2546.

Sosnovtsev, S. V., Belliot, G., Chang, K. O., Prikhodko, V. G., Thackray, L. B., Wobus, C. E., Karst, S. M., Virgin, H. W., IV & Green, K. Y. (2006). Cleavage map and proteolytic processing of the murine norovirus nonstructural polyprotein in infected cells. *J Virol* **80**, 7816–7831.

Spann, K. M., Collins, P. L. & Teng, M. N. (2003). Genetic recombination during coinfection of two mutants of human respiratory syncytial virus. *J Virol* **77**, 11201–11211.

Thackray, L. B., Wobus, C. E., Chachu, K. A., Liu, B., Alegre, E. R., Henderson, K. S., Kelley, S. T. & Virgin, H. W., IV (2007). Murine noroviruses comprising a single genogroup exhibit biological diversity despite limited sequence divergence. *J Virol* **81**, 10460–10473.

Thiry, E., Meurens, F., Muylkens, B., McVoy, M., Gogev, S., Thiry, J., Vanderplasschen, A., Epstein, A., Keil, G. & Schynts, F. (2005). Recombination in alphaherpesviruses. *Rev Med Virol* **15**, 89–103.

Tolskaya, E. A., Romanova, L. I., Blinov, V. M., Viktorova, E. G., Sinyakov, A. N., Kolesnikova, M. S. & Agol, V. I. (1987). Studies on the recombination between RNA genomes of poliovirus: the primary structure and nonrandom distribution of crossover regions in the genomes of intertypic poliovirus recombinants. *Virology* **161**, 54–61.

Vende, P., Le Gall, G. & Rasschaert, D. (1995). An alternative method for direct sequencing of PCR products, for epidemiological studies performed by nucleic sequence comparison. Application to rabbit haemorrhagic disease virus. *Vet Res* **26**, 174–179.

Wobus, C. E., Karst, S. M., Thackray, L. B., Chang, K. O., Sosnovtsev, S. V., Belliot, G., Krug, A., Mackenzie, J. M., Green, K. Y. & Virgin, H. W., IV (2004). Replication of *Norovirus* in cell culture reveals a tropism for dendritic cells and macrophages. *PLoS Biol* **2**, e432.

Wobus, C. E., Thackray, L. B. & Virgin, H. W., IV (2006). Murine norovirus: a model system to study norovirus biology and pathogenesis. *J Virol* **80**, 5104–5112.

Worobey, M. & Holmes, E. C. (1999). Evolutionary aspects of recombination in RNA viruses. *J Gen Virol* **80**, 2535–2543.

Zheng, D. P., Ando, T., Fankhauser, R. L., Beard, R. S., Glass, R. I. & Monroe, S. S. (2006). Norovirus classification and proposed strain nomenclature. *Virology* **346**, 312–323.